The Five-, Six- and Seven-Vertex Dicarbaboranes, Monocarbaborane Anions and Borane Dianions with *closo* Structures. Nuclear Spin-Spin Coupling Constants Calculated by DFT Methods

Bernd Wrackmeyer

Anorganische Chemie II, Universität Bayreuth, D-95440 Bayreuth, Germany

Reprint requests to Prof. Dr. B. Wrackmeyer. E-mail: b.wrack@uni-bayreuth.de

Z. Naturforsch. **60b,** 955 – 961 (2005); received June 13, 2005

Five-, six- and seven-vertex dicarbaboranes, carborane anions and borane dianions have been studied by DFT calculations at the B3LYP/6-311+G(d,p) level of theory, aiming at determining the indirect nuclear spin-spin coupling constants with an emphasis on $J(^{11}B,^{11}B)$, $J(^{13}C,^{11}B)$ and $J(^{13}C,^{13}C)$. The reasonable agreement with all experimental data suggests that the calculated data can be used in the discussion of the bonding situation in these cluster compounds, for which many coupling constants cannot be determined experimentally. The delocalisation of electron density is reflected by changes in both magnitude and sign of the coupling constants. The trend in the coupling constants between nuclei in antipodal positions points towards direct bonding interactions.

Key words: Boron Clusters, NMR, Coupling Signs, DFT Calculations

Introduction

One intriguing starting point of carborane chemistry in the late fifties has been the report on a compound with the composition $C_2B_3H_5$ **1a** [1], which had been obtained in very low yield. The properties of **1a** did not agree with those of other organoboranes and, although a classical structure could be suggested [2], non-classical bonding as in polyhedral boranes or borates seemed more likely. Thus, compound **1a** turned out to be the smallest member of a class of neutral deltahedral clusters (**A**; Scheme 1), the 1,5-dicarba-*closo*-pentaborane(5). Only a few years later, Köster *et al.* succeeded in the bench scale synthesis of peralkylated derivatives $C_2B_3R_5$ **1b** [3], for which an analogous structure was assigned. NMR studies of the parent compound **1a** [4] and the peralkylated derivatives **1b** [5] supported the structural assumptions. The mechanism of the formation of compounds **1b** was reinvestigated [6, 7], and the molecular structure of $C_2B_3Et_5$ was determined in the solid state [6, 8], confirming the non-classical bonding. The existence of potential isomers of **1** has not been confirmed. A substituted carborane anion **2b** is known [9], related to the unknown *closo*-$[1\text{-}CB_4H_5]^-$ **2a**. The borate dianion *closo*-$[B_5H_5]^{2-}$ **3a** as well as derivatives of **3a** are unknown.

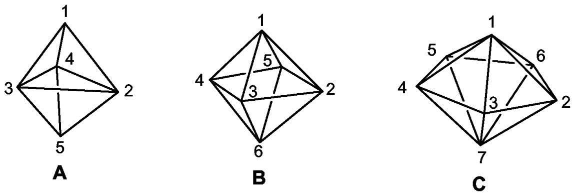

1a 1,5-$C_2B_3H_5$
2a $[1\text{-}CB_4H_5]^-$
3a $[B_5H_5]^{2-}$

4a 1,6-$C_2B_4H_6$
5a 1,2-$C_2B_4H_6$
6a $[CB_5H_6]^-$
7a $[B_6H_6]^{2-}$

8a 1,5-$C_2B_5H_7$
9a 1,2-$C_2B_5H_7$
10a 2,3-$C_2B_5H_7$
11a 2,4-$C_2B_5H_7$
12a $[1\text{-}CB_6H_7]^-$
13a $[2\text{-}CB_6H_7]^-$
14a $[B_7H_7]^{2-}$

Scheme 1. Schematic representation of the five-, six- and seven-vertex *closo* structures studied here.

The six- and seven-vertex closo-structures are represented by **B** and **C**, respectively (Scheme 1). There are two isomers known of *closo*-$C_2B_4H_6$, the 1,6-dicarba-*closo*-hexaborane(6) **4a** and the 1,2-dicarba isomer **5a** [10], and recently the hexaethyl derivative **4b** has been reported [11]. Although the carborane anion *closo*-$[CB_5H_6]^-$ **6a** has been proposed to be formed by deprotonation of *closo*-CB_5H_7 [12], it is poorly characterised so far, in contrast to the well-known [13] dianion *closo*-$[B_6H_6]^{2-}$ **7a**.

There are four isomers of $C_2B_5H_7$, 1,5-dicarba (**8a**), 1,2-dicarba- (**9a**), 2,3-dicarba- (**10a**), and 2,4-dicarba-

closo-heptaborane(7) **11a**, of which only **10a** and **11a** are known as the parent compounds [14, 15] or as derivatives [11, 16]. Two possible isomers of the carborane anion $[CB_6H_7]^-$ can exist, *closo*-$[1\text{-}CB_6H_7]^-$ **12a** and *closo*-$[2\text{-}CB_5H_7]^-$ **13a**, of which only the latter has recently been described [17]. The borane dianion *closo*-$[B_7H_7]^{2-}$ **14a** is known [18] as a fairly reactive species when compared with **7a**.

The bonding situation in these five- to seven-vertex clusters [19–21] should be mirrored by NMR parameters, in particular by nuclear spin-spin coupling constants involving the nuclei ^{11}B and ^{13}C [$^nJ(^{11}B,^{11}B)$, $^nJ(^{13}C,^{11}B)$ and $^nJ(^{13}C,^{13}C)$, in addition to $^1J(^{11}B,^1H)$ and $^1J(^{13}C,^1H)$]. However, owing to the quadrupolar nature of the ^{11}B nucleus ($I = 3/2$), and also because of the complex spin-systems present in all species **1–14**, experimental information on $^nJ(^{11}B,^{11}B)$, $^nJ(^{13}C,^{11}B)$ and $^nJ(^{13}C,^{13}C)$ is scarce, and experimental data $^1J(^{11}B,^1H)$ and $^1J(^{13}C,^1H)$ are not very accurate. The remarkable progress in the calculation of spin-spin coupling constants [22–25] encourages to apply theoretical methods to polyhedral compounds, and the small *closo*-clusters **1–14** can serve as instructive examples. Previous attempts in the application of Density-Functional-Theory (DFT) based on optimised molecular geometries (*e.g.* on the 6-311+G(d,p) or comparable level of theory) to boron compounds have met with success [26–28], and the agreement with experimental data, if available at all, has been satisfactory.

Results and Discussion

Comparison of experimental and calculated data

Numerous $^1J(^{11}B,^1H)$ values have been reported for polyhedral boron compounds [29, 30]. However, frequently these data are not accurate since the ^1H or ^{11}B resonance signals are broad and the complex spin systems have not been analysed. This is also true in most cases for the few $^1J(^{13}C,^1H)$ values [26, 31], although the influence of the complex spin-systems on these data is less important. Very few examples for coupling constants $^1J(^{11}B,^{11}B)$ in the frameworks of deltahedral boranes and carboranes have been measured, and the magnitude was found between less than 10 and 25 Hz [26, 30]. Coupling constants $^1J(^{13}C,^{11}B)$ and $^nJ(^{13}C,^{13}C)$ ($n = 2$) have been determined solely for the 1,5-dicarba-*closo*-pentaboranes(5) **1a** [4], **1b** [5], and **13b** [17], where ^{13}C labelling was used in the case of the parent compound **1a** [4] in order to measure $^2J(^{13}C,^{13}C)$. As shown in Scheme 2, there is good agreement between experimental and calculated coupling constants for **1a** and **1b**.

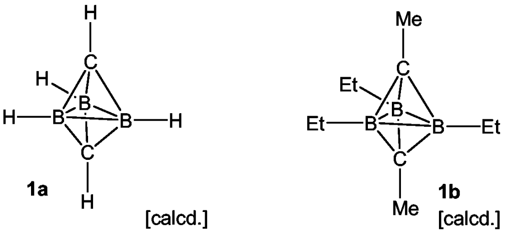

1a [calcd.]

$^1J(^{11}B,^1H)$ 189 [+182.3]
$^1J(^{13}C,^1H)$192 [+183.7]
$^1J(^{13}C,^{11}B)$ 18 [+20.5]
$^1J(^{11}B,^{11}B)$ n.m. [-0.6]
$^2J(^{13}C,^{13}C)$ 15 [+16.2]
$^3J(^{13}C,^1H)$ 19.8 [+18.8]
$^4J(^1H,^1H)$ .10.8 [+9.0]

1b [calcd.]

$^1J(^{13}C(1),^{13}C_{Me})$ 53 [+52.2]
$^1J(^{13}C_{Et},^{11}B)$ 78 [+68.6]
$^1J(^{13}C,^{11}B)$ 20 [+22.4]
$^1J(^{11}B,^{11}B)$ < 10 [-2.0]
$^2J(^{13}C,^{13}C)$ n.m. [+22.2]

Scheme 2. Comparison of experimental (n.m. means not measured) and calculated spin-spin coupling constants for 1,5-dicarba-*closo*-pentaboranes(5) **1a** [4] and **1b** [5]. In the case of **1b**, the experimental data have been measured for the 1,5-Me_2-2,3,4-Et_3-derivative, and calculated data are for 1,5-$C_2B_3Me_5$.

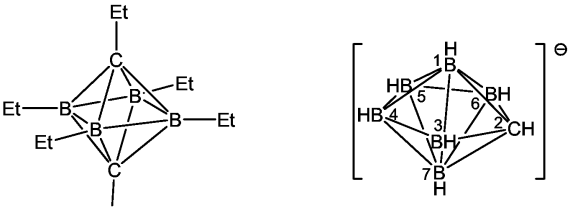

4b | **4b** (1,6-$C_2B_4Me_6$) [calcd.]

$^1J(^{13}C,^{11}B)$ <15 [+12.6]

13a [calcd.]

$^1J(^{13}C(2),^{11}B(3))$ 20 [+16.7]
$^1J(^{13}C(2),^{11}B(1))$ n.m. [+1.8]
$^2J(^{13}C(2),^{11}B(4))$ n.m. [+5.2]
$^1J(^{11}B(1),^1H)$ 151 [+137.7]
$^1J(^{11}B(3),^1H)$ 138 [+140.2]
$^1J(^{11}B(4),^1H)$ 150 [+135.1]
$^1J(^{13}C(2),^1H)$ n.m.[+157.0]

Scheme 3. Comparison of experimental (n.m. means not measured) and calculated spin-spin coupling constants for hexaalkyl-1,6-dicarba-*closo*-hexaborane(6) **4b** (experimental data for the hexaethyl and calculated data for the hexamethyl derivative), and for the 2-carba-*closo*-heptaborate(1$^-$) **13a**.

In principle, the information on $J(^{11}B,^{11}B)$, $J(^{13}C,^{11}B)$ and $J(^{13}C,^{13}C)$ in polyhedral boron compounds is present in the line width of the ^{11}B or ^{13}C NMR signals, for which the broadening can be traced to partially relaxed scalar ^{11}B-^{11}B and ^{13}C-^{11}B spin-spin coupling. However, it is difficult to extract

Table 1. Selected calculated coupling constants [Hz] for the five- to seven vertex boron clusters **1a – 14a**, and **1b** and **4b**.

	$^{1}J(^{11}B,^{1}H)$	$^{1}J(^{13}C,^{1}H)$	$^{1}J(^{11}B,^{11}B)$	$^{1}J(^{13}C^{11}B)$	$J(^{13}C,^{13}C)$	Other *J* values
1 a[a] 1,5-$C_2B_3H_5$	+182.3 (2)	+183.7(1)	-0.6 (2-3)	+20.5 (1-2)	+16.2 (1-5)	+18.8 (C1-H5) +9.0 (H1-H5)
1 b[a] 1,5-$C_2B_3Me_5$	+68.6 (2-$^{13}C_{Me}$)	+52.2 (1-$^{13}C_{Me}$)	-2.0 (2-3)	+22.2 (1-2)	22.7 (1-5)	–
2 a $[1\text{-}CB_4H_5]^{-}$	+148.2 (2) +138.3 (5)	+170.6	+1.4 (2-3) +23.3 (2-5)	+18.8	–	+18.0 (C1-B5) +2.0 (B5-H1) +16.5 (C1-H5) +6.2 (H1-H5)
3 a $[B_5H_5]^{2-}$	+124.7 (1) +128.4 (2)	–	+25.6 (1-2) +2.8 (2-3)	–	–	+20.6 (B1-B5) +14.1 (B1-H5) +3.4 (H1-H5)
4 a 1,6-$C_2B_4H_6$	+183.4 (2)	+175.9 (1)	+10.0 (2-3)	+12.4 (1-2)	+14.1 (1-6)	+5.0 (B2-B4) +13.4 (B2-H4) +21.1 (C1-H6) +11.7 (H1-H6)
4 b[b] 1,6-$C_2B_4Me_6$	75.7 (2-$^{13}C_{Me}$)	47.5 (1-$^{13}C_{Me}$)	+10.4 (2-3)	+12.6 (1-2)	+22.2 (1-6)	+9.9 (B2-B4)
5 a 1,2-$C_2B_4H_6$	+178.3 (3) +164.4 (4)	+190.2 (1)	+15.0 (3-4) +26.2 (4-6)	+7.4 (1-3) +8.4 (2-6)	-3.4 (1-2)	+6.5 (B1-B6) +12.7)B1-H6) +6.1 (H1-H6)
6 a $[CB_5H_6]^{-}$	+141.3 (2) +130,1 (6)	+161.1 (1) +20.2 (2-6)	+14.4 (2-3)	+8.9 (1-2)	–	+8.6 (B2-B4) +11.7 (C1-B6) +13.6 (B2-H4) +15.7 (B6-H1) +19.7 (C3-H6) +8.5 (H1-H6) +5.9 (H2-H4)
7 a[c] $[B_6H_6]^{2-}$	+114.9(1)	–	+18.1 (1-2)	–	–	+11.5 (B1-B6) +14.7 (B1-H6) +. . . (H1-H6)
8 a 1,7-$C_2B_5H_7$	+190.0 (2)	+189.9 (1)	+13.9 (2-3)	+6.1 (1-2)	+10.8 (1-7)	+1.7 (B2-B4) +20.9 (C1-H7) +14.1 (H1-H7)
9 a 1,2-$C_2B_5H_7$	+170.1 (3) +171.4 (4) +161.1 (7)	+180.3 (1) +179,8 (2)	+19.0 (3-4) +15.9 (4-5) +9.1 (3-7) +21.5 (4-7)	-2.0 (1-3) +2.9 (1-4) +15.7 (2-3) +0.1 (2-7)	-7.7 (1-2)	+3.5 (C1-B7) +9.8 (B7-H1) +18.7 (C1-H7) +10.7 (H1-H7)
10 a 2,3-$C_2B_5H_7$	+170.0 (1) +165.0 (4) +157.2 (5)	+180.9	+10.4 (1-4) +18.8 (1-5) +20.9 (4-5)	-2.4 (2-1) +19.7 (2-6)	+8.0 (2-3)	+1.5 (B1-B7) +5.7 (B4-B6) +4.8 (C2-B5) +10.1 (B1-H7) +8.3 (H1-H7)
11 a 2,4-$C_2B_5H_7$	+171.6 (1) +175.2 (3) +168.3 (5)	+175.0 (2)	+2.7 (1-3) +11.2 (1-5) +24.7 (5-6)	+5.3 (2-1) +29,6 (2-3) +14.3 (2-6)	+5.0 (1-3)	+1.0 (B1-B7) +2.0 (N3-B5) +9.2 (B1-H7) +7.9 (H1-H7)
12 a $[1\text{-}CB_6H_7]^{-}$	+145.4 (2) +129.7 (7)	+155.2 (1)	+17.1 (2-3) +16.7 (2-7)	+1.8 (1-2)	–	+3.8 (B2-B4) +4.5 (C1-B7) +11.2 (B7-H1) +20.5 (C1-H7) +10.9 (H1-H7)
13 a[b] $[2\text{-}CB_6H_7]^{-}$	+137.7 (1) +140.2 (3) +135.1 (4)	+157.0 (2)	+8.2 (1-3) +16.8 (1-4) +22.7 (3-4) +18.9 (4-5)	+1.8 (1) +16.7 (3)	–	+1.2 (B1-B7) +5.2 (C2-B4) +8.0 (B1-H7) +10.7 (H1-H7)
14 a $[B_7H_7]^{2}$	+114.2 (1) +116.9 (2)	–	+13.5 (1-2) +20.4 (2-3)	–	–	+1.8 (B1-B7) +6.0 (B2-B4) +12.1 (B1-H7) +6.8 (H1-H7)

[a] See also Scheme 2 for experimental data; [b] see also Scheme 3 for experimental data; [c] calculated data from ref. [28].

reliable data from the broadened NMR signals, considering that the relevant nuclei are often chemically equivalent and magnetically non-equivalent, giving rise to complex spin systems, and/or that the spin-spin coupling arises from several different interactions.

In the case of the hexaethyl-1,6-dicarba-*closo*-hexaborane(6) **4b**, we have measured a severely broadened ^{13}C(1,6) NMR signal [11]. Taking into account the relaxation rate of the ^{11}B nuclei [$T_1(^{11}\text{B}) \approx 0.01$ s], the magnitude of $^1J(^{13}\text{C},^{11}\text{B}) \leq 15$ Hz can be estimated [splitting of the ^{13}C NMR signal would become observable if $2\pi J(^{13}\text{C},^{11}\text{B})\text{T}_1(^{11}\text{B}) > 1$], This is in reasonable agreement (Scheme 3) with the calculated value $^1J(^{13}\text{C},^{11}\text{B}) = +12.6$ Hz for the hexamethyl derivative.

Rather different ^{13}C-^{11}B spin-spin coupling interactions are conceivable for the anion *closo*-$[2\text{-CB}_6\text{H}_7]^-$ **13b**, for which the ^{13}C NMR signal has been observed as a multiplet caused by $^1J(^{13}\text{C},^{11}\text{B}) \approx 20$ Hz. The pattern of the multiplet can be best explained as the result of spin-spin coupling between ^{13}C and two adjacent ^{11}B nuclei. Apparently, other potential one-bond or two-bond ^{13}C-^{11}B spin-spin coupling interactions are not resolved and cause only further broadening of the ^{13}C NMR signal. The calculations for **13b** (Scheme 3) indicate that the magnitude of the coupling constant $^1J(^{13}\text{C},^{11}\text{B}(3,6))$ is substantial (+16.7 Hz), whereas the other coupling constants $^1J(^{13}\text{C},^{11}\text{B}(1,7))$ and $^2J(^{13}\text{C},^{11}\text{B}(4,5))$ are much smaller (+1.8 Hz and +5.2 Hz, respectively).

In all cases where experimental data for coupling constants are available, the agreement with calculated data is reasonably good. Therefore, the calculated coupling constants for species which have not been studied experimentally or which are not accessible at all so far can be assumed to be meaningful. Table 1 lists the calculated one-bond and some long-range coupling constants for the compounds **1 – 14**.

The bonding situation in five- to seven-vertex clusters in the light of coupling constants

In a simplified approach, the cluster "σ bonding" results from the mutual overlap of the radial orbitals, one for each cluster atom, and the "π-bonding" arises from overlap of the tangential p orbitals, two for each cluster atom. The fourth orbital belonging to each cluster atom possesses high s character, similar to the radial orbital, and is engaged in the respective *exo*-B-H or C-H bond. This simple model predicts that n cluster atoms require $(2n+2)$ electrons to form a *closo*-structure, as shown in the electron counting rules [32]. The question of overlap, in particular of the tangential orbitals is important for the relative stability of the clusters and therefore, both the shape of the cluster and the origin of the orbitals (*e.g.* centred at boron or carbon) will have a significant influence [19 – 21].

For nuclei such as ^{1}H, ^{11}B and ^{13}C, the mechanism of spin-spin coupling interactions [33, 34] is dominated by the Fermi contact term (FC). Non-contact contributions from the spin-orbital term (SO) or the spin-dipole term (SD) are of minor importance in most cases (*vide infra* for exceptions), as it has been assumed [26] and is evident now from the calculations in this work. Thus, the magnitude of the coupling constants and also their sign depend on the s overlap integrals of the respective orbitals. The inspection of the data for the trigonal bipyramidal clusters **1 – 3** shows that the coupling constants $^1J(^{11}\text{B},^{11}\text{B})$ for the ^{11}B nuclei in the trigonal plane are small and even negative, in contrast with the coupling constants involving the ^{11}B nuclei in the plane and the ^{13}C or ^{11}B nuclei in the caps. In the six-vertex clusters, the magnitude of the coupling constants $^1J(^{11}\text{B},^{11}\text{B})$ in the tetragonal plane increases at the cost of the coupling interactions with the nuclei in capping positions. It is remarkable that in **5a** the sign of $^1J(^{13}\text{C},^{13}\text{C})$ is negative (-3.6 Hz), indicating a negligible σ bond character of the C-C bond [35]. This can be explained assuming that the s electron density donated by the carbon atoms to the cluster bonding is used almost entirely for the ^{13}C-^{11}B and ^{11}B-^{11}B spin-spin interactions, reflected by the rather large magnitude of $^1J(^{13}\text{C},^{11}\text{B})$ and $^1J(^{11}\text{B},^{11}\text{B})$. In the seven-vertex clusters, the overlap between tangential orbitals of capping atoms and those of the atoms in the corresponding pentagonal planes is less efficient than in the octahedral clusters. At the same time the s electron density in the radial orbitals is distributed between more atoms. This means that the magnitude *e.g.* of $^1J(^{13}\text{C}(1),^{11}\text{B}(2)$ in **8a** (+6.4 Hz) is much smaller than in **4a** (+12.1 Hz). The case **9a** is the second example for a negligible σ bond character of a bond between a capping carbon and a carbon atom in a plane [$^1J(^{13}\text{C}(1),^{13}\text{C}(2)) = -7.7$ Hz], and the reason is the same as for the analogous situation in **5a**. The sign of the coupling constant $^1J(^{13}\text{C}(2),^{13}\text{C}(3)) = +8.0$ Hz in **10a** is positive although its magnitude is still rather small, when compared with "normal" C-C single bonds [36]. Therefore, the spin-spin coupling interactions between the ^{11}B nuclei in the pentagonal plane should benefit from the s electron density provided by the carbon atoms. This is reflected *e.g.* by $^1J(^{11}B(4),^{11}B(5)) = +20.9$ Hz, similar to the comparable data for **13a** and **14a**.

In $^1J(^{13}C(2),^{13}C(3)) = +8.0$ Hz in **10a**, there is a substantial contribution from the paramagnetic spin-orbital term (PSO $= -4.5$ Hz) which is about half of the magnitude of the PSO term usually found for $^1J(^{13}C,^{13}C)$ of olefinic double bonds. In ethene, the PSO term has been connected with CC(pp)π bonding [37], in addition to the σ bond, for which the PSO contribution is small. Indeed, the C(2)-C(3) bond in **10a** can be considered a π bond with small σ bond character. Although for all other one-bond coupling constants between the heavy nuclei in **1**–**14** the PSO contributions are smaller, their sign is always negative in the range from -0.7 to -2 Hz and not to be neglected. By contrast, contributions from the spin-dipole term are small (SD < 0.1 Hz in most cases) and can be neglected. Both PSO and SD contributions are associated with energetically low-lying excited states which are not present in these *closo*-clusters.

Interactions between nuclei in antipodal positions in the closo-clusters

An important question regarding the *closo*-structures concerns bonding interactions between atoms in antipodal positions, which should be reflected by ^{11}B-^{11}B, ^{13}C-^{11}B or ^{13}C-^{13}C spin-spin coupling. Early experimental evidence for such coupling between ^{13}C nuclei has been presented in the case of **1a** [4], confirmed by the present and previous calculations [26] (Scheme 2). Since the spin-spin coupling between the antipodal nuclei is formally a two-bond coupling, the interactions can in principle be transmitted across several equivalent coupling pathways. However, then the magnitude of this type of coupling constants should increase with the number of coupling pathways in going from the five- to the seven-vertex clusters. The comparison between calculated $^2J(^{13}C,^{13}C)$ values for **1a** (16.2 Hz), **4a** (14.1 Hz), and **8a** (10.8 Hz) shows the opposite trend. Similar changes are calculated for the capping nuclei with $^2J(^{13}C,^{11}B)$ (**2a**, **6a**, **12a**) and $^2J(^{11}B,^{11}B)$ (**3a**, **7a**, **13a**, **14a**). The magnitude of these coupling constants is not related to the distance between the antipodal nuclei: the coupling constants become smaller, whereas the distances between the capping nuclei become shorter in going from the five- to the seven-vertex clusters. Therefore, it is concluded that the increasing number of atoms participating in the s electron density in the radial orbitals is responsible for the smaller magnitude of the antipodal "two-bond" couplings in the seven-vertex clusters. The positive sign, calculated for these coupling constants, also indicates that a direct through-bond interaction is more important than two-bond coupling pathways. Methyl groups as substituents at the cluster atoms should lead to an increase in the s electron density in the cluster. The calculations predict a large influence on the antipodal couplings in the permethylated derivatives **1b** and **4b**, where the magnitude of $^2J(^{13}C,^{13}C)$ increases by 6.1 and 8.1 Hz, respectively, in contrast to very small changes of the ^1J values. The analogous effect, although somewhat smaller (4.9 Hz), is observed for $^2J(^{11}B,^{11}B)$ in **4b**, when compared with **4a**. The distances between the antipodal carbon atoms in both **1b** and **4b**, or boron atoms in **4b**, are calculated to be slightly longer than in the parent compounds **1a** and **4a**.

The PSO and SD contributions to the antipodal ^2J values are small (< 1 Hz), but the sign of the PSO contribution has changed to positive (negative for all ^1J in the clusters), and the SD contributions to ^2J values (very small and almost negligible for ^1J in the clusters) are always positive and greater than those from the PSO term. This reminds of the changes in the sign and magnitude of PSO and SD in going from ethene to ethyne, except that the magnitudes of the respective terms are much smaller in the clusters. In ethane, for comparison, where the C-C bond can be considered as a bond with dominant σ character and where energetically low-lying excited states are absent, the calculation, at the same level of theory, shows that the PSO contribution to $^1J(^{13}C,^{13}C)$ is only $+0.01$ Hz and SD $= +1.1$ Hz, also very small when compared with the FC contribution of $+33.2$ Hz ($\Sigma = 34.3$; note the excellent agreement with the experimental value of 34 Hz).

Conclusions

The reasonable agreement between experimental and calculated spin-spin coupling constants for nuclei forming *closo*-clusters is encouraging to further use the calculated data in the discussion of the bonding situation in known or still unknown cages with *closo* structures. The electron delocalisation in these electron-deficient species causes smaller magnitudes of the ^1J values when compared with data for ${}^1J({}^{11}B,{}^{11}B)$ [30, 38, 39] ${}^1J({}^{13}C,{}^{11}B)$ [27, 31] and ${}^1J({}^{13}C,{}^{13}C)$ [36] typical of 2e/2c bonds. The calculated negative sign of some values ${}^1J({}^{13}C,{}^{13}C)$ is indicative of a small s overlap integral of the C-C bonds. The trends in the spin-spin coupling interactions between antipodal nuclei are more readily explained by direct bonding rather than by two-bond coupling pathways. In comparison with the Fermi contact term, the non-contact contributions to the spin-spin coupling, although small, cannot be neglected. The trends in these non-contact terms are opposite for the ${}^1J$ and antipodal ${}^2J$ values.

Experimental Section

The Gaussian 03 program package [40] served for all optimisations of the gas phase geometries for the compounds **1** – **14**, using DFT methods (B3LYP) [41] and the 6-311+G(d,p) basis set [42]. The optimised geometries were characterised as minima (absence of imaginary frequencies) on the respective potential energy surface by calculating analytically the frequencies of the stationary points. In the case of **1b**, the X-ray structural analysis has been carried out for the pentaethyl derivative and the calculations were done for the pentamethyl compound. The agreement betweeen experimental and calculated structural data is shown in Table 2.

Table 2. Comparison of experimental[a] and calculated structural data for **1b** (X-ray structural analysis for 1,5-$C_2B_3Et_5$ [6, 8] and calculation for 1,5-$C_2B_3Me_5$).

1,5-$C_2B_3R_6$	Bond lengths [pm] exp.	calcd.		Bond angles [°] exp.	calcd.
C(1)-C(5)	227.5	225.3	B-C-B	73.2	73.7
C(1)-B(2,3,4)	156.9	156.3	C-B-C	92.3	92.3
B – B	187.7	187.3			

[a] Mean distances and angles.

The spin-spin coupling constants for all clusters **1** – **14** were calculated for the optimised geometries at the same level of theory [B3LYP/6-311+G(d,p)]. As in previous work [27, 28], it was observed that the most consistent results were obtained with the B3LYP method. The significance of the different contributions (FC, SO, SD) to the spin-spin coupling constants, which are experimentally inaccessible, was investigated carefully. In the case of the spin-orbital contribution (SO), only the paramagnetic spin-orbital term (PSO) was found to be of appreciable magnitude, whereas the diamagnetic spin-orbital term (DSO) was negligible (< 0.1 Hz) in all cases studied. Various reasons for deviations between experimental and calculated data, in particular when ${}^1H$ nuclei are involved, have been discussed previously [26].

Acknowledgement

Support of this work by the Deutsche Forschungsgemeinschaft is gratefully acknowledged.

[1] a) I. Shapiro, C. D. Good, R. E. Williams, J. Am. Chem. Soc. **84**, 3837 (1962); b) R. N. Grimes, Carboranes, Academic Press, New York (1970).
[2] M. Hofmann, M. A. Fox, R. Greatrex, P. v. R. Schleyer, J. W. Bausch, E. A. Williams, Inorg. Chem. **35**, 6170 (1996).
[3] a) R. Köster, G. W. Rotermund, Tetrahedron Lett. 1667 (1964); b) R. Köster, H.-J. Horstschäfer, P. Binger, P. K. Mattschei, Liebigs Ann. Chem. 1339 (1975).
[4] T. Onak, E. Wan, J. Chem. Soc. Dalton Trans. 665 (1974).
[5] R. Köster, B. Wrackmeyer, Z. Naturforsch. **36b**, 704 (1981).
[6] R. Köster, R. Boese, B. Wrackmeyer, H.-J. Schanz, Chem. Commun. 1691 (1995).
[7] a) B. Wrackmeyer, H.-J. Schanz, W. Milius, Angew. Chem. **109**, 98 (1997); Angew. Chem. Int. Ed. Engl. **36**, 75 (1997); b) B. Wrackmeyer. H.-J. Schanz, Coll. Czech. Chem. Commun. **62**, 1254 (1997).
[8] M. Antipin, R. Boese, D. Bläser, A. Maulitz, J. Am. Chem. Soc. **119**, 326 (1997).
[9] Y. Sahin, C. Präsang, M. Hofmann, G. Geiseler, W. Massa, A. Berndt, Angew. Chem. **117**, 1670 (2005); Angew. Chem. Int. Ed. **44**, 1643 (2005).
[10] I. Shapiro, B. Keilin, R. E. Williams, C. D. Good, J. Am. Chem. Soc. **85**, 3167 (1963).
[11] B. Wrackmeyer, H.-J. Schanz, W. Milius, C. McCammon, Collect. Czech. Chem. Commun. **64**, 977 (1999).
[12] a) S. R. Prince, R. Schaeffer, J. Chem. Soc. Chem. Commun. 451 (1969); b) J. Jaballas, T. Onak, J. Organomet. Chem. **550**, 102 (1998).
[13] W. Preetz, G. Peters, Eur. J. Inorg. Chem. 1831 (1999).
[14] R. R. Rietz, R. Schaeffer, J. Am. Chem. Soc. **95**, 6254 (1973).
[15] T. P. Onak, F. J. Gerhart, R. E. Williams, J. Am. Chem. Soc. **85**, 3373 (1963).
[16] a) Z. J. Abdou, G. Abdou, T. Onak, S. Lee, Inorg. Chem. **25**, 2678 (1986); b) J. S. Beck, A. P. Kahn, L. G. Sneddon, Organometallics **5**, 2552 (1986).
[17] B. Štibr, O. L. Tok, W. Milius, M. Bakardjiev, J. Holub, D. Hnyk, B. Wrackmeyer, Angew. Chem. **114**, 2230 (2002); Angew. Chem. Int. Ed. **41**, 2126 (2002).
[18] T. Klanberg, G. R. Eaton, L. J. Guggenberger, E. I. Muetterties, Inorg. Chem. **6**,1271 (1967).
[19] E. D. Jemmis, J. Am. Chem. Soc. **104**, 7017 (1982).
[20] P. v. R. Schleyer, K. Najafian, Inorg. Chem. **37**, 3454 (1998).

[21] E. D. Jemmis, P. D. Pancharatna, Appl. Organomet. Chem. **17**, 480 (2003).

[22] a) V. Sychrovsky, J. Gräfenstein, D. Cremer, J. Chem. Phys. **113**, 3530 (2000); b) J. E. Peralta, G. E. Scuseria, J. R. Cheeseman, M. J. Frisch, Chem. Phys. Lett. **375**, 452 (2003).

[23] T. Helgaker, M. Jaszunski, K. Ruud, Chem. Rev. **99**, 293 (1999).

[24] R. H. Contreras, V. Barone, J. C. Facelli, J. E. Peralta, Annu. Rep. NMR Spectrosc. **51**, 167 (2003).

[25] a) L. B. Krivdin, S. P. A. Sauer, J. E. Peralta, R. H. Contreras, Magn. Reson. Chem. **40**, 187 (2002); b) L. B. Krivdin, Magn. Reson. Chem. **42**, 500 (2004).

[26] T. Onak, J. Jaballas, M. Barfield, J. Am. Chem. Soc. **121**, 2850 (1999).

[27] B. Wrackmeyer, A. Berndt, Magn. Reson. Chem. **42**, 490 (2004).

[28] B. Wrackmeyer, Z. Naturforsch. **58b**, 1192 (2004).

[29] a) G. R. Eaton, W. N. Lipscomb, NMR Studies of Boron Hydrides and Related Compounds, W. A. Benjamin Inc, New York (1969); b) W. Jarvis, Z. J. Abdou, T. Onak, Polyhedron **2**, 1067 (1983).

[30] a) A. R. Siedle, Annu. Rep. NMR Spectrosc. **20**, 205 (1988); b) D. Kennedy, in J. Mason (ed.), Multinuclear NMR, pp. 221 – 258, Plenum Press, New York (1987).

[31] B. Wrackmeyer, Progr. NMR Spectrosc. **12**. 227 (1979).

[32] a) K. Wade, Adv. Inorg. Chem. Radiochem. **18**, 1 (1976); b) R. E. Williams, Adv. Inorg. Chem. Radiochem. **18**, 67 (1976); c) R. E. Williams, Chem. Rev. **92**, 177 (1992).

[33] N. F. Ramsey, Phys. Rev. **91**, 303 (1953).

[34] C. J. Jameson, in J. Mason (ed.) Multinuclear NMR, pp. 89 – 131, Plenum Press, New York (1987).

[35] M. D. Newton, J. M. Schulman, M. M. Manus, J. Am. Chem. Soc. **96**, 17 (1974).

[36] a) K. Kamienska-Trela, in E. Buncel, J. R. Jones (eds.): Isotopes in the Physical and Biomedical Sciences, Vol. 2, pp. 297 – 365, Elsevier, Amsterdam (1991); b) K. Kamienska-Trela, Annu. Rep. NMR Spectrosc. **30**, 131 (1995); c) V. Wray, Progr. NMR Spectrosc. **13**, 177 (1979).

[37] D. Cremer, E. Kraka, A. Wu, W. Luettke, ChemPhysChem **5**, 349 (2004).

[38] F. Bachmann, H. Nöth, H. Pommerening, B. Wrackmeyer, T. Wirthlin, J. Magn. Reson. **34**, 237 (1979).

[39] P. Greiwe, A. Bethäuser, H. Pritzkow, Th. Kühler, P. Jutzi, W. Siebert, Eur. J. Inorg. Chem. **2000**, 1927.

[40] Gaussian 03, Revision B.02, M. J. Frisch, G. W. Trucks, H. B. Schlegel, G. E. Scuseria, M. A. Robb, J. R. Cheeseman, J. A. Montgomery (Jr.), T. Vreven, K. N. Kudin, J. C. Burant, J. M. Millam, S. S. Iyengar, J. Tomasi, V. Barone, B. Mennucci, M. Cossi, G. Scalmani, N. Rega, G. A. Petersson, H. Nakatsuji, M. Hada, M. Ehara, K. Toyota, R. Fukuda, J. Hasegawa, M. Ishida, T. Nakajima, Y. Honda, O. Kitao, H. Nakai, M. Klene, X. Li, J. E. Knox, H. P. Hratchian, J. B. Cross, C. Adamo, J. Jaramillo, R. Gomperts, R. E. Stratmann, O. Yazyev, A. J. Austin, R. Cammi, C. Pomelli, J. W. Ochterski, P. Y. Ayala, K. Morokuma, G. A. Voth, P. Salvador, J. J. Dannenberg, V. G. Zakrzewski, S. Dapprich, A. D. Daniels, M. C. Strain, O. Farkas, D. K. Malick, A. D. Rabuck, K. Raghavachari, J. B. Foresman, J. V. Ortiz, Q. Cui, A. G. Baboul, S. Clifford, J. Cioslowski, B. B. Stefanov, G. Liu, A. Liashenko, P. Piskorz, I. Komaromi, R. L. Martin, D. J. Fox, T. Keith, M. A. Al-Laham, C. Y. Peng, A. Nanayakkara, M. Challacombe, P. M. W. Gill, B. Johnson, W. Chen, M. W. Wong, C. Gonzalez, J. A. Pople, Gaussian, Inc., Pittsburgh PA (2003).

[41] a) A. D. Becke, J. Chem. Phys. **98**, 5648 (1993); b) C. Lee, W. Yang, R. G. Parr, Phys. Rev. B **41**, 785 (1988); c) P. J. Stevens, F. J. Devlin, C. F. Chablowski, M. J. Frisch, J. Phys. Chem. **98**, 11623 (1994).

[42] a) D. McLean, G. S. Chandler, J. Chem. Phys. **72**, 5639 (1980); b) R. Krishnan, J. S. Binkley, R. Seeger, J. A. Pople, J. Chem. Phys. **72**, 650 (1980).